ACCOUNTS OF CHEMICAL RESEARCH

VOLUME 3 NUMBER 12 DECEMBER, 1970

Ion–Molecule Collision Processes

BRUCE H. MAHAN

Inorganic Materials Research Division of the Lawrence Radiation Laboratory and Department of Chemistry, University of California, Berkeley, California 94720

Received July 16, 1970

In an earlier article[1] I described the motivation, execution, and first results of our experiments in which a collimated, mass analyzed ion beam of known energy impinges on a scattering gas and the distribution of velocity vectors of the charged products of ion–molecule reactions is measured. Our immediate object in this work is to deduce from the measured product energy and angular distributions information about the details of the reaction dynamics. Our long-term goal is to use this information to test calculated potential energy surfaces for the systems investigated.

As a given bimolecular elementary chemical reaction ordinarily occurs, reactant molecules distributed over many different internal and translational quantum states undergo collisions which range from head-on to grazing. Certain of these collisions produce product molecules distributed in an unknown way over a variety of internal and translational energy states. The measured rate constant for reaction represents the result of an average of the "detailed" rate constants for reaction of molecules in particular quantum states, using the Boltzmann factor to give the relative importance of each of the individual detailed rate constants. Since the measured, or phenomenological, rate constant stands as one number representing the average effect of a vast variety of collision processes, very little about the details of any of these reaction processes can be drawn from it. We can say that all this information has been lost in the averaging process or that an apparatus which measures only the rate at which products appear completely ignores the details of how they appear.

In order to learn more about reaction dynamics, experiments must be done in which the reactants are confined to a somewhat restricted range of quantum states, and some fairly detailed measurement of the condition of newly formed products is made. In the molecular beam method, this is accomplished by using beam collimation and speed selection to restrict the velocity vectors of reactants and by using energy and angle selective detectors to measure the distribution of the magnitude and direction of product velocity vectors.

We can understand the principle of our ion beam scattering experiments easily if we recognize that the velocity vector which describes the motion of a projectile ion relative to a target molecule represents the initial state of the combined target–projectile system about to undergo a transition. The ion beam part of our apparatus is a device which "prepares" the composite system in a known initial state, that is, a chemically identified ion moving relative to an identified target in a known direction at a known speed. The detector of the apparatus analyzes the state of the target–projectile system after the collision by determining the mass and velocity vector of the scattered ion. From these measured final and initial mass and velocity states and the laws of conservation of energy and momentum, the internal energy of the collision partners and the deflection produced by the collision can be calculated.

The interaction which causes these transitions is the intermolecular potential sampled by the colliding molecules along their trajectories. Even when the initial velocity vector is very well defined, a very large variety of collisions can occur which sample rather different regions of the intermolecular potential. These collisions differ in the value of the *impact parameter* or aiming error, which is the distance by which the center of mass of the molecules would miss each other if no intermolecular forces operated.

The way in which variation of the impact parameter affects the collision trajectory can be discerned readily. Figure 1 shows a potential energy surface for the interaction of two atoms. We can see what would happen in an elastic nonreactive collision between a moving projectile and a stationary target by imagining the motion of a frictionless point particle on this surface. Trajectories which correspond to small, medium, and large impact parameter collisions are shown in the figure. The initial and final states of the system are represented by the straight-line motion of the particle on the flat parts of the surface, while the transitions from initial to final states are produced by the curved parts of the surface which represent long-range attraction and short-range repulsion between the atoms.

In a nearly head-on (small impact parameter) collision, the centers of the projectile and target approach until virtually the entire initial kinetic energy is converted to potential energy. At this "turning point" the collision partners reverse their relative motion and

(1) B. H. Mahan, *Accounts Chem. Res.*, 1, 217 (1968).

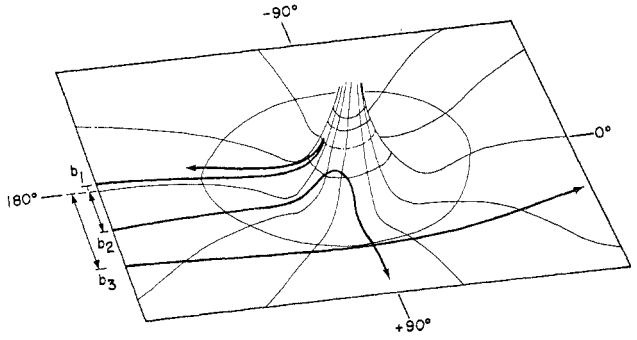

Figure 1. A representation of the potential energy between a fixed target atom and a projectile atom as a function of their internuclear separation. Representative trajectories are shown for cases in which the aiming error or impact parameter b of the projectile is small, medium, and large. The scattering angle in a collision is measured from the original direction of the projectile to the final straight-line portion of its trajectory. Note that the curvature of the trajectory, and hence the scattering angle, is principally determined by the behavior of the projectile near the distance of closest approach to the target.

start to recede from each other, thereby acquiring their final relative velocity vector. For these nearly head-on collisions, the final relative velocity vector makes a large angle with the initial relative velocity vector (180° for an exactly head-on collision). It is the potential energy surface in regions where the kinetic energy is smallest (that is, near the distance of closest approach or turning point) that is most responsible for the details of what happens in these small impact parameter collisions. Thus we have the convenient association that small impact parameter collisions give large angle scattering whose details are determined by the "close" target–projectile configurations in which the potential energy is nearly equal to the initial relative kinetic energy.

When the impact parameter is large, that is, of the order of a typical bond distance or greater, the target and projectile undergo a grazing collision in which the potential energy is never large compared to the initial kinetic energy. Thus the intermolecular forces which act are not large, and the final relative velocity vector makes only a small angle with the initial relative velocity vector. We have therefore another convenient association: large impact parameter collisions sample the outer regions of the potential surface and give small angle scattering.

Of course, in systems capable of chemical reaction, the intermolecular potential energy is a function of at least three interatomic coordinates, and the unrestricted motion of the system in all degrees of freedom is very difficult or impossible to visualize. In addition, the fact that mass is transferred between target and projectile clouds our intuitive picture of a reactive collision trajectory. However, trajectories for reactive collisions have much in common with those from elastic collisions. It is virtually always true that as long as the initial relative translational energy in a reactive collision is comparable to or greater than chemical bond energies, we can make the association between large impact parameters, grazing collisions, and small angle scattering and between small impact parameters, intimate collisions, and large angle scattering. These associations can fail when the energy of collision is small and when the colliding molecules attract each other strongly, but this failure can be recognized from the experiments and is in fact an occurrence with its own intrinsic interest.

In an actual experiment, all values of the impact parameter occur, and in general scattering is expected at all angles relative to the ion beam. By measuring the intensity of scattering as a function of angle and making use of the associations just discussed, we can deduce qualitatively what type of collision is responsible for the various dynamical processes of elastic, inelastic, and reactive scattering.

The first systems we studied[1-5] by this ion beam–product velocity vector method were exothermic hydrogen or deuterium atom transfer reactions as in eq 1–4.

$$N_2^+ + D_2 \longrightarrow N_2D^+ + D \quad (1)$$

$$N_2^+ + CH_4 \longrightarrow N_2H^+ + CH_3 \quad (2)$$

$$Ar^+ + D_2 \longrightarrow ArD^+ + D \quad (3)$$

$$N^+ + H_2 \longrightarrow NH^+ + H \quad (4)$$

While the details of the product distributions and, therefore, the reaction dynamics differed significantly, there were several important features common to all distributions which led to the following general deductions. When the relative energy of collision is 4 eV or greater, these exothermic atom-transfer reactions proceed by a "direct" interaction mechanism; that is, they involve a collision complex which lasts less than a full molecular rotational period (10^{-12}–10^{-13} sec at these energies). Grazing collisions in which the product ions proceed in much the same direction as the projectile ions make the principal contribution to the total reaction cross section. However, nearly head-on collisions in which the product ion is scattered through large angles are almost as important as grazing collisions, particularly at high energies.

The molecular ion products of these reactions are highly excited internally, often to their dissociation limit, and a major factor in determining the reaction probability at high energies is the necessity of forming product ions which are stable with respect to dissociation. Very large isotope effects occur which increase with increasing energy and always favor pick-up of H over D in grazing collisions by factors of up to 20. For more nearly head-on collisions in the N_2^+–HD system, the isotope effect favors the formation of N_2D^+ when the relative energy is near 4 eV and favors N_2H^+ when the relative energy is 8 eV or above.

The interpretation of these data in terms of potential energy surfaces is still at a very rudimentary level. Recently, however, Suplinskas[6] has calculated the velocity

(2) W. R. Gentry, E. A. Gislason, Y. T. Lee, B. H. Mahan, and C. W. Tsao, *Discuss. Faraday Soc.*, **44**, 137 (1967).
(3) W. R. Gentry, E. A. Gislason, B. H. Mahan, and C. W. Tsao, *J. Chem. Phys.*, **49**, 3058 (1968).
(4) E. A. Gislason, B. H. Mahan, C. W. Tsao, and A. S. Werner, *ibid.*, **50**, 142 (1969).
(5) M. Chiang, E. A. Gislason, B. H. Mahan, C. W. Tsao, and A. S. Werner, *ibid.*, **52**, 2698 (1970).
(6) T. F. George and R. J. Suplinskas, private communication.

vector distribution of ArD^+ from the Ar^+–D_2 reaction using classical mechanics and a potential energy surface based on the assumption that the atoms interact through a long-range ion–induced dipole attraction and a hard-sphere repulsion. The agreement between experiment and the calculated distribution obtained from this admittedly crude but qualitatively reasonable potential is very good.

There is an important lesson contained in the success of this crude potential surface. Even though scattering experiments give us much more detailed information about reaction dynamics than we have ever had, they still do not provide sufficient information to allow determination of the complicated three or more particle potential energy surface with a high accuracy. This observation, which has been all too easy to overlook, should come as no surprise. The much simpler job of finding an accurate intermolecular potential for two rare gas atoms has occupied many workers for many years, and still remains an active research area.

Even though current experiments permit us to make only qualitative conclusions about the gross features of potential surfaces, we can be very optimistic about future possibilities. The energy and angular resolution of the apparatus and the data analysis techniques now used can be greatly improved, and, as this is done, the more subtle aspects of potential surfaces will start to emerge. In the meantime, beam experiments can give us firm answers to many long-standing qualitative questions in chemical kinetics. In this article I will relate some of the recent results obtained in my laboratory which we feel elucidate the processes of excitation of molecular vibrations, the collisional dissociation of molecules, and the behavior of relatively long-lived or sticky collision complexes.

Collisional Excitation of Molecular Vibration

Before a molecule can decompose or rearrange it must acquire internal energy as vibrational motion. Conversely, a molecule formed by combination of two smaller fragments must have some of its vibrational energy removed before it becomes stable to redissociation or other unimolecular processes. Consequently, the collisional transfer of vibrational energy to and from a molecule is an important kinetic process, and a great deal of effort has gone into its study, both experimentally and theoretically.[7-9]

There are methods[7] of determining vibrational–translational energy-exchange rates which depend on measuring a macroscopic property like the velocity of sound, or the low-pressure (second-order) limit of the rate constant of a pseudounimolecular reaction. These methods give an energy-exchange rate which is an average over different kinds of vibrational transition, over all types of collision from grazing to head-on, and over the Boltzmann distribution of relative molecular velocities. Even more specific techniques like the quenching of laser-induced fluorescence[9] yield a rate averaged over the complete spread of velocities and the full range of impact parameters. Fortunately, ion-beam techniques allow us to discern the difference in the effectiveness of head-on and more nearly grazing collisions in producing vibrational excitation and to do this in experiments in which the relative velocity of the collision partners is fairly well defined and variable over a wide range. In the past year, my research group has performed many such experiments and gained increased understanding of the vibrational excitation process. Somewhat similar ion-beam-vibrational excitation studies have been done in the laboratories of Toennies,[10] Datz,[11] and Moran.[12]

Figure 2 shows a contour map of the intensity of NO^+ scattered by a helium gas target. A polar coordinate system is used in which the radial coordinate is the speed of NO^+ relative to the center of mass of the NO^+–He system. (The velocity of the target–projectile center of mass is constant throughout any type of collision and is therefore a natural origin.) The other coordinate, the so-called center-of-mass scattering angle, is the angle between the initial and final relative velocity vectors and is measured with respect to the original direction of the NO^+ projectile. Consequently, the NO^+ ions only slightly deflected by grazing collisions appear at angles less than 90°, while those which have made more nearly head-on collisions appear at large scattering angles.

An elastic collision is one in which the *speed* of the NO^+ ion relative to the center of mass is the same after the collision as before, even though the direction of the trajectory is altered. Therefore, the locus of elastically scattered NO^+ is a circle with a radius equal to the initial speed of the projectiles relative to the center of mass. This circle is labeled $Q = 0$ in Figure 2. The quantity Q is the difference between final and initial relative energies of the collision partners, is zero when no energy is transferred into internal modes of motion, and is negative for inelastic collisions where the final relative translational energy and speed must be less than those initially.

We can see in Figure 2 that at small (<60°) scattering angles the maximum in the ridge of scattered intensity coincides with the elastic circle. Therefore, grazing collisions in which the intermolecular potential is small compared to the initial kinetic energy are essentially elastic in nature. In contrast, for angles greater than 90°, the intensity maximum lies off the elastic circle, closer to the origin. Since these particles scattered through large angles have speeds smaller than that of the projectile ions, they must have undergone inelastic collisions which produced internal excitation. Thus the appearance of Figure 2 can be interpreted qualitatively as follows. There are a large number of grazing collisions which produce small-angle scattering which is essentially elastic. The increase in the inelasticity

(7) B. Stevens, "Collisional Activation in Gases," Pergamon Press, Oxford, England, 1967.
(8) D. Rapp and T. Kassal, *Chem. Rev.*, **69**, 61 (1969).
(9) C. B. Moore, *Accounts Chem. Res.*, **2**, 103 (1969).
(10) J. Schöttler and J. P. Toennies, *Z. Phys.*, **214**, 472 (1968).
(11) P. F. Dittner and S. Datz, *J. Chem. Phys.*, **49**, 1969 (1968).
(12) T. F. Moran and P. C. Cosby, *ibid.*, **51**, 5724 (1969).

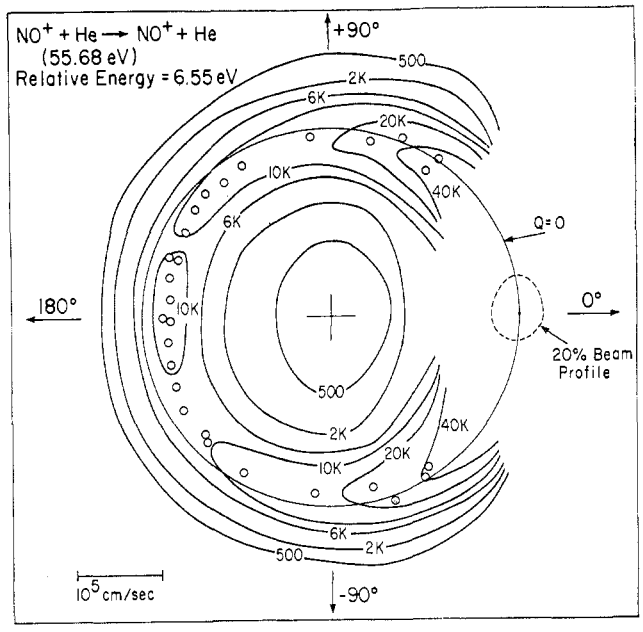

Figure 2. A contour map of the specific intensity of NO^+ scattered from He at an initial relative energy of 6.55 eV. The polar coordinate system has as its origin the velocity of the NO^+–He center of mass, the radial coordinate is the speed of NO^+ relative to the center of mass, and the angular coordinate is the scattering angle in the center of mass system, measured with respect to the direction of the initial ion beam. The circle labeled $Q = 0$ is the locus of the velocity of NO^+ scattered elastically. The small circles locate points of maximum intensity and thus represent the most probable speed at a particular angle.

which occurs at larger scattering angles indicates that head-on collisions are more effective in producing internal excitation than are grazing collisions.

The maximum inelasticity in Figure 2 occurs near 180° and corresponds to 1.4 eV appearing as internal energy of the products. Neither NO^+ nor He has excited electronic states with energies this small, so the internal energy must be present either as vibration and/or rotation of NO^+. In a nearly head-on collision, very little torque can be exerted by He on NO^+, and consequently we do not expect rotational excitation to be produced by such collisions. We conclude that for scattering near 180° virtually all the internal excitation goes into vibration of NO^+. In contrast, scattering near 90° and at smaller angles involves grazing collisions in which torques occur, and rotational excitation very probably occurs along with vibrational excitation. Consequently, we have concentrated on studying the scattering near 180°, which can be meaningfully interpreted in terms of pure vibrational excitation.

Because of the low resolution of our apparatus, excitations to individual vibrational levels are not resolved. The inelasticity of 1.4 eV corresponding to the intensity maximum at 180° in Figure 2 does give us the most probable vibrational excitation energy, however. Since the vibrational energy level spacing of NO^+ is 0.29 eV, the most probable change in vibrational quantum number in this experiment was 4 or 5. We have observed that even larger quantum number changes occur in collisions with high relative translational energy. There has been a tendency to overlook or discount the possibility of such large changes in quantum number, since most other experimental techniques involve or are sensitive to only small changes. However, various theories[8] have predicted these large vibrational quantum number changes. They are observed in our experiments because they occur only when the relative kinetic energy of collision is in the 2- to 20-eV range, and at present only ion-beam techniques can explore this energy region with any facility.

Our measurements of the vibrational excitation of NO^+ and O_2^+ in head-on collisions with He are nicely in agreement with a slightly modified version of the classical theory of vibrational excitation proposed by Landau and Teller[13] in 1935. This theory treats a one-dimensional collinear collision in which the target atom interacts with the nearest atom of the diatomic molecule *via* a repulsive potential of the form $V = V_0 e^{-r/L}$. Here r is the distance between interacting atoms of the target and projectile, V_0 is a constant which does not appear in the final expression for the transferred energy, and L is a length parameter, usually about 0.2 Å, which determines how rapidly the potential energy rises as the atoms approach each other. The theoretical expression[14] for the energy ΔE transferred into vibration is

$$\Delta E = E_{rel}[4M_A M_B M_C/(M_A + M_B)^2 \times (M_B + M_C)^2](\pi\omega L/v_0)^2 \operatorname{csch}^2(\pi\omega L/v_0) \quad (5)$$

Here M_A is the mass of the target atom, M_B is the mass of the atom in the diatomic which hits the target, M_C is the mass of the trailing atom of the diatomic, ω is the circular vibrational frequency, and E_{rel} and v_0 are respectively the initial relative energy and relative speed of the target and projectile. When M_B and M_C are different but of similar magnitude, as is the case in NO^+, each may be replaced by their average without appreciable error.

Equation 5 shows that the transferred energy is a function of the factor in brackets which involves only the atomic masses, and also of the dimensionless group $\pi\omega L/v_0$. Since L is a characteristic length over which the potential energy changes substantially, and v_0 is a speed characteristic of relative motion, $v_0/\pi L = \omega_c$ is a "frequency" which characterizes the rate at which the intermolecular potential changes during the collision. Therefore, the amount of energy transferred into vibrational depends, apart from mass factors, only on ω/ω_c, the ratio of the vibrational frequency to the "disturbing" frequency. The ratio of internal to perturbing frequency is an ubiquitous factor in inelastic collision theories for all types of excitation. When this factor is small, the energy transferred, or the transition probability, is large, and *vice versa*. This is nicely illustrated by eq 5 since, as v_0 increases, ω/ω_c approaches zero, the product of the last two factors in eq 5 approaches unity, and, depending on the mass factor, the change in vibrational energy can be a substantial fraction of E_{rel}. In

(13) L. Landau and E. Teller, *Phys. Z. Sowjetunion*, **10**, 34 (1936).
(14) B. H. Mahan, *J. Chem. Phys.*, **52**, 5221 (1970).

contrast, as ω/ω_c increases, the hyperbolic cosecant is closely approximated by $\exp(-\omega/\omega_c)$, and the energy transferred becomes exponentially small.

Figure 3 shows a comparison between eq 5 and our experimental data. The agreement between theory and experiment is very good over the complete range of initial energies studied. Of course, the theory does include the parameter L, but this was not adjusted to fit our data. Instead, it was chosen *a priori* according to a potential energy curve matching procedure[15] which relates L to the Lennard-Jones potential parameters of NO^+ and He. We[16] have found similarly good agreement between our experimental results for O_2^+ and N_2^+ collisions with He. It is worth remarking that the substantial disagreement of our data with a conventional form of classical vibration energy transfer theory led us to discover a long-standing inconsistency in the theory. When this inconsistency in the treatment was removed,[14] good agreement between experiment and theory resulted. Thus, at least for collision partners which have a combination of atomic masses similar to those in the systems we have investigated, the simple corrected analytical classical theory of vibrational energy transfer works very well indeed for high-energy collisions.

This pleasing result should not be interpreted as a complete vindication of the classical theory and exponential repulsive potential. The theory strictly applies only to head-on collinear collisions, whereas in the scattering at 180° the collisions are head-on, but the atoms are not necessarily collinear. Furthermore, a much more searching test of the intermolecular potential could be made if excitations to individual vibrational states could be resolved. We have experiments in which we hope to accomplish this resolution now under way.

Collisional Dissociation of Molecules

In elementary treatments of chemical kinetics, the collisional dissociation of a diatomic molecule is written as a simple, one-step process, for example

$$Br_2 + Ar \longrightarrow Br + Br + Ar$$

The implication is that, if Br_2 and Ar collide with a relative translational energy equal to or greater than the bond energy of Br_2, a dissociation will certainly occur. Indeed, at any one temperature the measured rates at which such processes occur are approximately equal to $Z\exp(-D/kT)$, that is, to the total collision rate Z multiplied by a Boltzmann factor in which the activation energy is equal to the bond energy D. On the other hand, we have just seen that even in the most favorable case of head-on collision only approximately 25% of the initial relative translational energy is converted to internal excitation in an NO^+–He collision. This makes it seem quite unlikely that dissociation could occur upon every collision which met the minimum energy requirement. Therefore the one-step or strong collision description of dissociation may not be an accurate description of what occurs in nature.

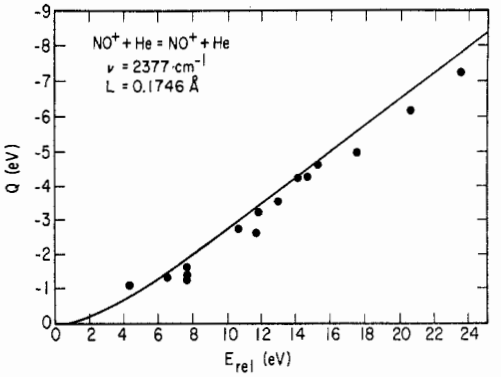

Figure 3. The exothermicity (or negative inelasticity) Q as a function of initial relative energy for 180° scattering in the NO^+–He system. The circles are experimental data, while the curve is the prediction of eq 5 with the parameters given.

There is another possibility.[17] The dissociation of diatomics could occur as a result of a many-step collisional excitation–deactivation process in which molecules gradually work their way up the ladder of vibrational states and are finally dissociated from a highly excited level by a rather weak collision. There is support for the occurrence of this ladder-climbing mode of dissociation both from theoretical calculations and macroscopic dissociation rate measurements.

We have determined the importance of the strong single collision mode of dissociation in several systems with our ion-beam apparatus.[18] Figure 4 shows the velocity vector distribution of O^+ from the reaction

$$O_2^+ + He \longrightarrow O^+ + O + He$$

at a relative energy of 8.31 eV. The maximum intensity of O^+ occurs at a velocity very nearly equal to the velocity of O_2^+ before the collision. Thus it appears that in many collisions one oxygen atom is stripped out of the molecule by collision with helium while the other proceeds freely, having experienced a relatively small impulse or disturbance during the dissociation. As the collision energy is increased, this description becomes less accurate, and both dissociation fragments are scattered broadly.

The most significant feature of Figure 4 is that the total intensity of the O^+ fragment ion is very small, even though the initial relative energy of 8.31 eV is 2.5 eV (57 kcal/mole) in excess of the bond energy of O_2^+. Thus, the strong collision mode of dissociation indeed seems to be a rather improbable process, even when there is more than sufficient energy available. This qualitative assessment is confirmed by the results given in Table I, where we list the cross sections for dissociation in O_2^+–He and NO^+–He collisions at various energies. For comparison, the total cross section for elastic,

(15) K. F. Herzfeld and T. A. Litovitz, "Absorption and Dispersion of Ultrasonic Waves," Academic Press, New York, N. Y., 1959, p 282.

(16) M. H. Cheng, M. H. Chiang, E. A. Gislason, B. H. Mahan, C. W. Tsao, and A. S. Werner, *J. Chem. Phys.*, **52**, 6150 (1970).

(17) D. L. Bunker, "Theory of Elementary Gas Reaction Rates," Pergamon Press, Oxford, England, 1966, Chapters 3 and 4.

(18) M. H. Cheng, M. H. Chiang, E. A. Gislason, B. H. Mahan, C. W. Tsao, and A. S. Werner, *J. Chem. Phys.*, **52**, 5518 (1970).

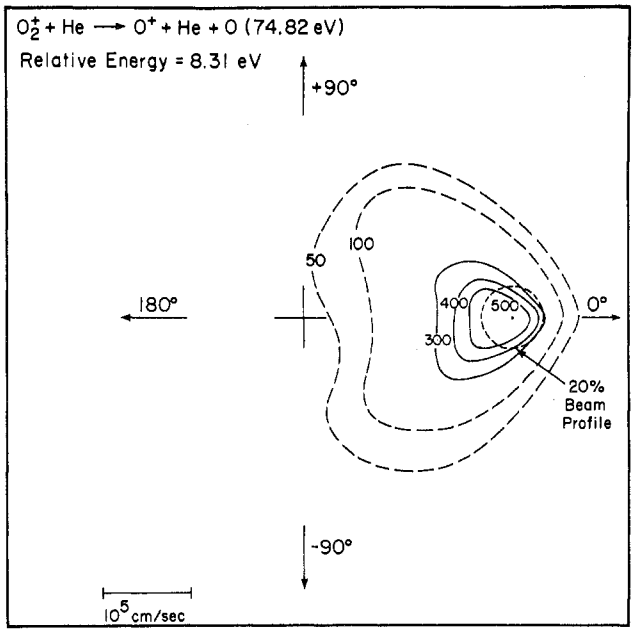

Figure 4. A contour map of the specific intensity of O^+ from O_2^+–He collisions at an initial relative energy of 8.31 eV. The dashed contours are somewhat uncertain because of very low intensity. The intensity maximum lies at a velocity slightly smaller than the velocity of the primary beam particles.

Table I
Total Cross Sections for Dissociation

System	E_{rel}, eV	σ, Å²
$O_2^+ \rightarrow O^+$	8.32	0.013
	11.1	0.054
	16.5	0.1
	16.5	0.23
	19.4	0.83
	19.4	0.83
	27.7	1.5
$NO^+ \rightarrow O^+$	23.6	0.12
$NO^+ \rightarrow N^+$	17.7	0.054
$N_2O^+ \rightarrow O^+$	12.5	0.49
$N_2^+ \rightarrow N^+$	18.7	0.056

inelastic, and dissociative scattering should be approximately $\pi\sigma^2$, where σ is the Lennard-Jones size parameter. This gives a total cross section of approximately 28 Å². The fact that the dissociation cross sections given in Table I are much smaller than this shows that only a small fraction of collisions produces dissociation even when the available energy is well in excess of the bond dissociation energy.

When helium is replaced by a target of greater mass, the dissociation cross sections increase, but not by a large increment. The small cross sections which we have found lead to rate constants for dissociation which are much smaller than those measured experimentally. Therefore, it seems clear that the one-shot strong collision mechanism is not an important contributor to the dissociation of diatomic molecules and that the overwhelming fraction of dissociations occur by variants of the ladder-climbing mechanism.

Chemical Reactions

We have already pointed out that the exothermic atom-transfer reactions 1–4 have in common several characteristics of their product velocity vector distributions. These similarities suggest that the major features of the potential energy surfaces for the reactions are very much alike. After completing work on reactions 1–4, we wished to examine a system which had a rather different potential energy surface and which, therefore, would have different reaction dynamics and display a new type of product velocity vector distribution. Reaction 6 seemed to have all the properties we

$$O_2^+ + D_2 \longrightarrow DO_2^+ + D \qquad (6)$$

required. It is endothermic by 1.9 eV, a substantial amount. Even more important, the ion $D_2O_2^+$ is known[19] to be a stable species, with a net binding energy of 2.6 eV with respect to the reactants O_2^+ and D_2. Thus it was clear that there would be a deep well in the potential surface. We strongly suspected that this potential well would lead to the occurrence of relatively long-lived collision complexes, rather than the very short-lived complexes observed in the N_2^+–D_2 reaction. Finally, the O_2^+–D_2 system had the interesting feature that several different sets of products are possible, in addition to those of reaction 6

$$O_2^+ + D_2 \longrightarrow OD^+ + OD$$
$$O_2^+ + D_2 \longrightarrow D_2O^+ + O$$
$$O_2^+ + D_2 \longrightarrow O^+ + O + D_2$$

Other reactions can also occur, but these are the ones which we have investigated in detail.

Figure 5 shows a contour map of the intensity of DO_2^+ from collisions in which the initial relative kinetic energy (2.76 eV) is rather low. It should be compared with the distribution of N_2D^+ from the N_2^+–D_2 reaction shown in Figure 6. The significant feature of the DO_2^+ distribution is that it is symmetric about a line through $\pm 90°$ in the center-of-mass coordinate system. Such a symmetry indicates that the reactants collide to form a "sticky" complex which rotates many times and then dissociates randomly with the products leaving in a direction which is uncorrelated with the direction of the projectile ion beam. In contrast, the distribution of N_2D^+ is very asymmetric about the $\pm 90°$ line, with the greatest product intensity in the small-angle region. This asymmetry indicates that the N_2^+ which leaves the complex as N_2D^+ "remembers" the direction it had as it entered the collision region. This correlation between product and reactant velocity vectors implies a collision complex which exists for less than one molecular rotational period. Thus the N_2D^+ and DO_2^+ distributions are very different, with the DO_2^+ showing the influence of a deep potential well associated with the $D_2O_2^+$ complex.

There are other experimental data which confirm the existence of a long-lived complex in the O_2^+–D_2 system. We[20] measured the velocity vector distributions of HO_2^+ and DO_2^+ from low-energy (<4 eV) O_2^+–HD collisions and found that both isotopic products were distributed

(19) J. L. Franklin, *et al.*, *Nat. Stand. Ref. Data Ser., Nat. Bur. Stand.*, No. 26 (1969).
(20) E. A. Gislason, B. H. Mahan, C. W. Tsao, and A. S. Werner, *J. Chem. Phys.*, **50**, 5419 (1969).

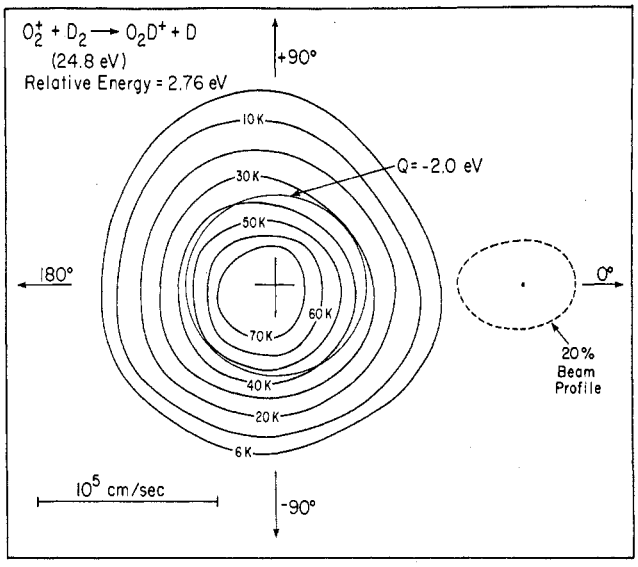

Figure 5. An intensity contour map of DO_2^+ formed from O_2^+–D_2 collisions at 2.76-eV relative energy. The nearly isotropic distribution of intensity about the center of mass velocity indicates that the formation of DO_2^+ proceeds through a long-lived $D_2O_2^+$ collision complex.

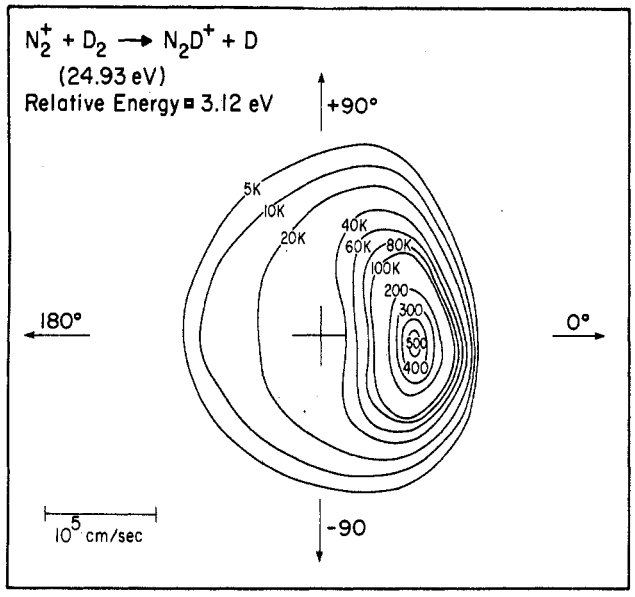

Figure 6. An intensity contour map of N_2D^+ formed from N_2^+–D_2 collisions at 3.12-eV initial relative energy. The distribution is asymmetric about the ±90° line, with an intensity maximum in the small-angle region. This indicates that, in the most probable reactive event, N_2^+ picks up a D atom in a short-lived grazing collision with D_2, and the resulting N_2D^+ proceeds in approximately the same direction as the original projectile motion.

symmetrically about the ±90° line in the center-of-mass system. Moreover, the DO_2^+ was in much greater abundance than HO_2^+. This is also what is expected from the decay of a long-lived complex. The strong atomic interactions in such complexes should lead to products whose intensities are proportional to their intrinsic statistical weights. The ion DO_2^+ has a lower zero-point energy than HO_2^+, and because of its lower vibration frequencies it has a greater density of internal energy states. Therefore, it should be formed in greater abundance than HO_2^+ in the statistical decay of the HDO_2^+ complex, just as is observed. Finally, a calculation of the lifetime of $D_2O_2^+$ with respect to dissociation to DO_2^+ was made, using the Rice–Ramsperger–Kassel–Marcus (RRKM) theory of unimolecular reactions.[17] The result found was that $D_2O_2^+$ formed in collisions with less than 4-eV relative energy should live longer than ten molecular rotations before dissocating to products. Despite the several approximations and assumptions necessary to the execution of this calculation, the qualitative finding that long-lived complexes should be observed at these low collision energies is reassuring.

From unimolecular reaction rate theory, it is expected that the lifetime of a complex will decrease as its internal energy increases. In ion-beam experiments we can change the internal energy of the complex by changing the relative translational energy of the collision partners. We would expect that, as the collision energy is increased, the lifetime of the complex should decrease to less than one rotational period, and the symmetry of the product angular distribution about the ±90° line should be lost. We undertook such experiments in order to see how accurately the RRKM theory could predict the collision energy at which the lifetime of the complex became less than one rotational period.

Figure 7 shows a contour map of the intensity of

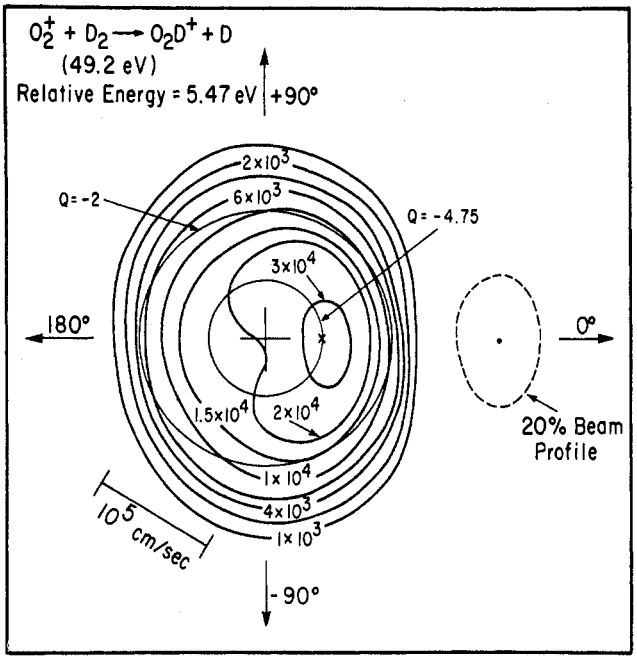

Figure 7. An intensity contour map of DO_2^+ from O_2^+–D_2 collisions at 5.47-eV relative energy. The intensity distribution is now asymmetric about the ±90° line, which indicates that the reaction proceeds through a short-lived direct interaction at this and higher initial relative energies. The small cross marks the velocity of products formed by the ideal stripping mechanism, while the circles marked $Q = -2$ and -4.75 give the limits of product speeds which are imposed by reaction endothermicity and product instability, respectively. Finite resolution of the apparatus and motion of the target gas are responsible for product intensity outside the $Q = -2$ eV circle, and inside the $Q = -4.75$ eV circle.

DO_2^+ formed by O_2^+–D_2 collisions at a relative energy of 5.5 eV. The appearance of an intensity maximum in

the small-angle region indicates that at this relative energy the lifetime of many of the complexes is of the order of one rotation or less. The lifetime of the complex calculated by RRKM theory is of the order of three rotations. At this stage, this must be considered to be very encouraging agreement. Most of the molecular parameters of $D_2O_2^+$ necessary for the calculation had to be estimated, and no account was taken of the fact that the $D_2O_2^+$ complex has several modes of decay available to it. If this latter factor were taken into account, the calculated lifetime of the complex would decrease by a factor which could easily be 3 or more. Moreover, it is probably not reasonable to expect the statistical unimolecular decay theory to predict the lifetime of the complex accurately at an energy where the assumption of a statistical decay of a long-lived complex is starting to fail. We expect that further studies of the lifetimes of collision complexes and the velocity distribution of their decomposition products will reveal to us the validity of current unimolecular decay theories and point out what changes must be made to improve them.

The behavior of the velocity distribution of H_2O^+ from O_2^+–H_2 collisions is similar to that just described for DO_2^+. When the initial relative energy is low, H_2O^+ has an isotropic distribution of velocities symmetric about the center of mass velocity origin. At higher energies, the distribution of H_2O^+ is asymmetric and indicates that the reaction occurs through a short-lived interaction in which an O^+ is stripped out of the O_2^+ projectile to form H_2O^+, while the freed O atom receives a relatively small impulse. The extreme process[1] in which the freed O atom receives no impulse and seems merely to observe as the O^+ is stripped away is called "spectator stripping." Thus the $O_2^+(H_2,O)H_2O^+$ undergoes a transition from a long-lived complex to something akin to spectator stripping as the relative energy of collision is increased.

The distribution of OH^+ from O_2^+–H_2 collisions is symmetric about $\pm 90°$ in the center of mass system when the initial relative energy is low. This certainly would be expected if OH^+ were being formed by decay of the same long-lived $H_2O_2^+$ complex that produces HO_2^+ and H_2O^+. However, this symmetry of the OH^+ distribution persists even when the relative collision energy is so high (10 eV) that no long-lived complex could exist, and formation of HO_2^+ and H_2O^+ clearly occurs by impulsive processes. This persistent symmetry of the OH^+ distribution is very probably a consequence of the near identity of the product partners OH^+ and OH. Since these molecules differ merely by exchange of an electron, there is no reason to expect that even at the highest energies the OH^+ will be scattered preferentially either at angles greater or less than 90°, as long as the collision proceeds through an intermediate which has equivalent oxygen atoms. Thus our observance of a highly symmetric OH^+ distribution at all collision energies indicates that the collision intermediate $H_2O_2^+$ which forms OH^+ resembles hydrogen peroxide rather than a linear OOHH or T-shaped $OO\begin{matrix}H\\H\end{matrix}$ structure.

As indicated earlier, the isotope effects in low-energy O_2^+–HD collisions agree qualitatively with the predictions of unimolecular reaction theory. More interesting isotope effects occur when the energy is high enough so that the complex is short lived. Figure 8 shows the distributions of HO_2^+ and DO_2^+ from an O_2^+–HD collision at 8.6 eV. The HO_2^+ is scattered in the small-angle region almost exclusively, while the DO_2^+ appears at larger angles. This is the first such extreme anisotropy in an isotope effect to be observed, although a milder angular dependence of an isotope effect had been discovered by us[3] in the N_2^+–HD system.

There is probably no single explanation for the extreme angular dependence of the HO_2^+/DO_2^+ isotope effect, but there are at least three simple possibilities which may contribute. The first is that the HDO_2^+ collision complex will tend to be formed with O_2^+ and HD roughly parallel to each other, and perpendicular to the direction of flight of the O_2^+. The fact that the center of mass of the resulting $HOOD^+$ is closer to the D atom than to the H atom will, on the average, cause the complex to start to rotate with the OH end moving in the flight direction of the O_2^+ projectile and the OD end moving oppositely. If the complex decomposes in less than one rotation, as it does in this high-energy regime, any HO_2^+ formed will tend to be traveling in the forward, or small-angle, direction, whereas any DO_2^+ will be aimed into the large-angle region. Thus the explanation involves the fact that the centers of mass and of charge of HD are not coincident, and that therefore in general O_2^+–HD collisions are accompanied by a rotation of the complex which initially carries the H end in the direction of the projectile.

The second possible explanation for the angular dependence of the isotope effect involves the problem of stabilizing the incipient HO_2^+ or DO_2^+ molecule to decomposition to O_2^+ and an H or D atom. At a given laboratory kinetic energy, a projectile has a greater energy relative to a deuterium atom than to a hydrogen atom. Thus it is possible for O_2^+ at a laboratory energy of 100 eV to form stable HO_2^+ from HD by essentially a spectator stripping reaction with no necessity of dissipating the internal energy of HO_2^+ by recoil off the free deuterium atom. On the other hand, DO_2^+ formed by a spectator stripping process at the same projectile laboratory energy has enough internal energy to decay to O_2^+ and D. Thus DO_2^+ will not appear in the forward or small-angle region because such "stripped" DO_2^+ is unstable. If DO_2^+ is formed by collisions in which it rebounds off the free hydrogen atom, the product can be stabilized and will appear at large angles in the center-of-mass system. At the present time, we feel that this product stabilization process is the most likely cause of the anisotropy in the HO_2^+–DO_2^+ isotope effect at high energies.

The third possible reason for the anisotropic isotope effect involves the interconversion of the orbital angular momentum $\mathbf{L}$ associated with the approach of reactants to each other to the final rotational angular momentum $\mathbf{J}'$ of the DO_2^+ or HO_2^+ molecules and the final orbital

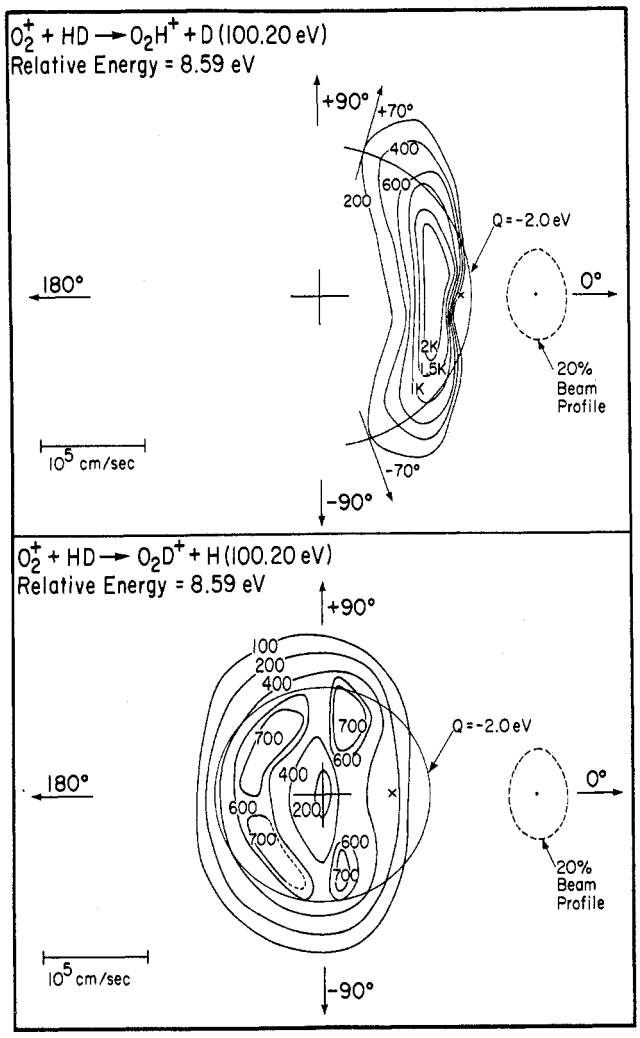

Figure 8. Contour maps of the intensities of products from the O_2^+–HD reactions at 8.59-eV relative energy. The upper panel shows the HO_2^+ product which is apparently formed by a direct interaction which gives predominantly forward scattered HO_2^+. The small cross locates the velocity of products formed by the ideal stripping process. The lower panel shows the velocity vector distribution of DO_2^+, again from O_2^+–HD collisions at 8.59-eV relative energy. The intensity lies principally in the large angle region, with only small amounts of DO_2^+ product at the ideal stripping velocity. In both maps, the product intensity lies closer to the center of mass than would be predicted by the ideal stripping or elastic spectator model.

angular momentum $\mathbf{L}'$ associated with the separation of the products. Since the rotational angular momentum $\mathbf{J}$ of the reactant molecules is small and can therefore be neglected in comparison with $\mathbf{L}$, we can write the approximate conservation law $\mathbf{L} \cong \mathbf{L}' + \mathbf{J}'$ which must hold for each reaction.

Now the initial and final orbital angular momenta $\mathbf{L}$ and $\mathbf{L}'$ are proportional respectively to the reduced mass of the reactants and products. For the reaction of O_2^+ with HD, the reactant reduced mass is close to 3 amu, the mass of the lighter of the two particles. Similarly, the reduced mass of $O_2H^+ + D$ is nearly 2 amu, and that of $O_2D^+ + H$ is nearly 1 amu. When the reduced mass of the products is much smaller than that of reactants, as is true when O_2D^+ and H are formed, we will have $\mathbf{L}' \ll \mathbf{L}$, so that $\mathbf{J}'$ will have to be large in order to conserve angular momentum. If the potential energy surface does not have strong angle-dependent forces which allow the product to be set into rapid rotation, then the reaction will not occur if $\mathbf{L}$ is large, but may occur if $\mathbf{L}$ is small. Since small values of $\mathbf{L}$ are associated with small impact parameters, we expect large angle scattering in this case. This is just what is found for DO_2^+ from O_2^+ on HD.

When the product of the O_2^+–HD collision is $HO_2^+ + D$, the reduced masses of reactants and products are more nearly comparable, and thus $\mathbf{L} \cong \mathbf{L}'$. There is, therefore, no necessity for converting large amounts of orbital angular momentum into rotation of HO_2^+, and thus the reaction can proceed even when $\mathbf{L}$ and the impact parameter are large. Consequently, we expect HO_2^+ to be scattered at small angles, as is observed experimentally.

Concluding Remarks

Ion-beam investigations of collision phenomena are still in their exploratory, low-resolution stage. Nevertheless, it is clear that even these crude initial experiments can provide clear qualitative answers to some of the classical questions of chemical kinetics. With the second generation of high-resolution apparatuses now in sight, we can anticipate much more detailed tests of the theories of vibrational and electronic excitation, unimolecular decomposition, and bimolecular reaction.

It is a pleasure to acknowledge the work of Drs. E. A. Gislason, C. W. Tsao, and M. H. Cheng, and Messrs. M. H. Chiang and A. S. Werner, who performed the experiments which I have discussed. I also acknowledge a discussion with Professor D. R. Herschbach which helped clarify some ideas concerning angular momentum disposal. The work was supported by the U. S. Atomic Energy Commission.